J. Plasma Physics (1998), *vol.* 60, *part* 4, *pp.* 775–786. Printed in the United Kingdom

Solar-energy liberation from water by electric arcs

GEORGE HATHAWAY,[1] PETER GRANEAU[2] and NEAL GRANEAU[3]

[1] Hathaway Consulting Services, 39 Kendal Avenue, Toronto, Ontario, Canada M5R 1L5
[2] Center for Electromagnetics Research, Northeastern University, Boston, MA 02115, USA
[3] Department of Engineering Science, Oxford University, Parks Road, Oxford OX1 3PJ, UK

(Received 16 December 1997 and in revised form 27 May 1998)

This paper reports progress in an experimental investigation, started in the Hathaway laboratory in 1994, dealing with the liberation of intermolecular bond energy from ordinary water by means of an arc discharge. Photographic evidence of fog generation and explosion during the arcing period is included. A new fog accelerator is described and a table of results of the kinetic energies of fog jets is provided. A renewable water energy cycle is outlined. The fog kinetic energy has been found to be greater than the difference between the capacitor input energy and the heat losses. Given energy conservation, the only external energy input that can account for the fog kinetic energy is solar heat from the atmosphere.

1. Introduction

Früngel (1948) discovered the working principle of water arc launchers. The arc was established in a small cavity between a vertical rod electrode and a coaxial ring electrode by the discharge of a capacitor. The unusual strength of the explosions led to the development of a new technology known as electro-hydraulic metal forming (Wilson 1964). It was clearly recognized from the start that water arcs were relatively cold and no steam was created. Measurements of arc explosion forces were started at MIT (Graneau and Graneau 1985), in 1985 and continued at Northeastern University (Azavedo *et al.* 1986). On one occasion (Graneau and Graneau 1996), a 3.6 g water mass, travelling at approximately 1000 m s^{-1} punched a half-inch diameter hole through a quarter-inch thick aluminium plate. Not until 1993 was it realized that the water arc liberated energy from a source other than the capacitor input energy. This led Hathaway Consulting Services to resume experimentation with water arcs. The present paper describes a series of experiments that forms part of this continuing research programme.

The principal discovery made in the past three years was that it is a collection of fog droplets in the water that explodes, and not the liquid water itself. The term 'fog' stands for a multitude of tiny water droplets floating in air. Progress made in this research up to 1 October 1995 has been extensively reviewed in a recently published book (Graneau and Graneau 1996). Further information is

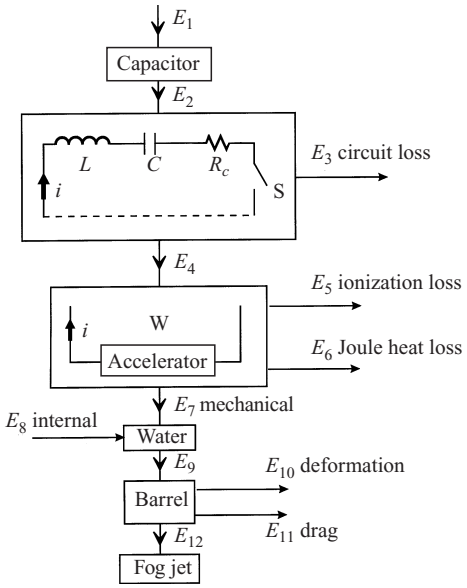

Figure 1. Energy flow diagram.

contained in a paper presented at the 1996 World Renewable Energy Congress (Graneau 1996).

In the reviewed experiments (Graneau and Graneau 1996), the energy delivered to small quantities of water (up to 1.5 ml) was typically less than 50 J (E_2 in Fig. 1). This could not have increased the water temperature by more than 10 °C, which is in agreement with measurements. Steam explosions were out of the question, because no liquid breakdown mechanism is known that can channel a significant fraction of the current into a thin water filament. It has to be remembered that the ionization process absorbs energy and does not generate heat.

As shown in the energy flow diagram of Fig. 1, the energy E_2 is discharged from the capacitor C into a simple series circuit comprising a switch S, the inductance L, the short-circuit resistance R_c and the water-filled cavity or accelerator W. The discharge current i is of the form

$$i = I_0 e^{-t/T} \sin \omega t, \tag{1}$$

where I_0 is the intercept of the exponential envelope with the current axis. T is the damping time constant, $\omega = 2\pi f$, where f is the ringing frequency, and t stands for time. From the current oscillogram, we can determine T and the damping factor R given by standard circuit theory as

$$R = \frac{2L}{T}. \tag{2}$$

R has two components:

$$R = R_0 + \frac{e_b}{i_{\mathrm{rms}}}. \tag{3}$$

R_0 is the Ohmic resistance of the discharge circuit and the water, and thus accounts for the total heat loss. The induced back-e.m.f. e_b in the water

https://doi.org/10.1017/S0022377898007089 Published online by Cambridge University Press

accounts for any mechanical work E_7 that has to be done on the water to generate cold fog. Unfortunately, we know of no way in which the components of (3) can be measured separately. Hence it is not possible to be precise about E_7.

E_7 must supply the surface-tension energy increase required by fog formation and, in addition, it may accelerate the droplets a small amount. This has to be achieved by either electrodynamic Lorentz or Ampère forces. The Lorentz pinch force can produce thrust in the direction of current flow. Northrup (1907) proved that the pinch thrust will be of the general electrodynamic form

$$F_7 = \frac{\mu_0}{4\pi}\frac{1}{2}i^2. \tag{4}$$

This holds for all conductor diameters.

E_{12} is the kinetic energy of the fog jet as it leaves the accelerator. The impulse that this jet exerts on an absorbing balsa-wood secondary projective has been measured (Graneau and Graneau 1996), and is given by

$$P_{12} = \int F_{12}\,dt = mu_{\mathrm{av}}, \tag{5}$$

where F_{12} is the force, m is the mass of the fog and u_{av} is its average velocity. This should be compared with the mechanical impulse received by the fog droplets from the electrodynamic impulse P_7.

We may write

$$P_7 = \int F_7\,dt = \frac{\mu_0}{4\pi}k\int i^2\,dt, \tag{6}$$

where k is a numerical constant. The value of the action integral $\int i^2\,dt$ is available from the current oscillogram. To compare P_{12} with P_7, we express P_{12} as

$$P_{12} = \frac{\mu_0}{4\pi}k'\int i^2\,dt, \tag{7}$$

and, using (5),

$$k' = 10^7\frac{mu_{\mathrm{av}}}{\int i^2\,dt}. \tag{8}$$

The dimensionless factor k' is now an experimentally determined quantity.

When water arc explosion forces were measured over ten years ago (Azavedo *et al.* 1986), it was found that $1000 < k' < 7000$. This fact has been confirmed in all subsequent experiments. It left little doubt that the water arc explosions contained additional energy E_8 over and above E_7, which was likely to be energy stored in the water.

When Ampère's force law is used in (6), the predicted k values increased from 0.5 (see (4)) to about 200 (Graneau and Graneau 1996). This is still far too small to deny the existence of internally stored water energy E_8, and gives an impulse ratio $P_{12}/P_7 = k'/k$ of the order of 50–100.

Provided that the impulses act on the same mass (fog), Newtonian mechanics then requires that

$$\frac{E_{12}}{E_7} = \left(\frac{P_{12}}{P_7}\right)^2. \tag{9}$$

https://doi.org/10.1017/S0022377898007089 Published online by Cambridge University Press

This can be proved as follows. If a mass m is accelerated to the velocity v_a, it requires an impulse of

$$P_a = \int F_a \, dt = m v_a. \tag{10}$$

Let the same mass acquire additional energy in flight to reach the velocity v_b; then the full impulse becomes

$$P_b = m v_b. \tag{11}$$

Therefore the impulse ratio is

$$\frac{P_b}{P_a} = \frac{v_b}{v_a}. \tag{12}$$

This makes the ratio of final to initial kinetic energy

$$\frac{E_b}{E_a} = \frac{\frac{1}{2} m v_b^2}{\frac{1}{2} m v_a^2} = \left(\frac{P_b}{P_a}\right)^2, \tag{13}$$

which proves (9).

For the impulse ratios of 50–100 of the water arc experiments (Graneau and Graneau 1996), this implies that E_{12} is at least 1000 times larger than E_7. We therefore claim that virtually all the kinetic energy of the fog jet leaving the water plasma accelerator is derived from the internal water energy contribution E_8.

2. Ionization of water

A normal plasma consists of an ionized gas. Liquids break down under high electric stress without first forming a gas phase, because electron avalanches can propagate in liquids and readily ionize the molecules to form an arc plasma. Arcs in water have been investigated quite extensively. They form the basis of a technology known as electro-hydraulic metal forming (Wilson 1964).

Pure water is a good dielectric, and breakdown is difficult to achieve. Saltwater and tapwater are more easily ionized (Azavedo *et al.* 1986) because of an electrolytic conduction phase that wastes much of the energy supplied to the water without producing any ions. The experiments described in this paper were therefore performed with distilled water.

Ionization losses occur in the arc of the switch S of Fig. 1 and in the water. A certain degree of ionization has to be established in both arcs before the discharge current can begin to flow. This causes a voltage drop on the capacitor terminals. The determination of this loss is discussed in Graneau and Graneau (1996). As a rule, it amounts to no more than approximately 10% of the input energy E_2. Further ionization losses will accumulate during current flow. In electrical circuit measurements they are indistinguishable from Joule and other current-damping losses. However, it is important to remember that ionization stores electrostatic energy and does not contribute to plasma heating. The stored energy is later regained as heat when the ions recombine. Figure 2 is an oscillogram of the discharge current and the voltage across the accelerator terminals. In this case the capacitor was charged to 11 kV. Before breakdown, but after the closure of the switch S, the full capacitor voltage is applied across the water insulation. When this breaks down, the voltage falls sharply because

https://doi.org/10.1017/S0022377898007089 Published online by Cambridge University Press

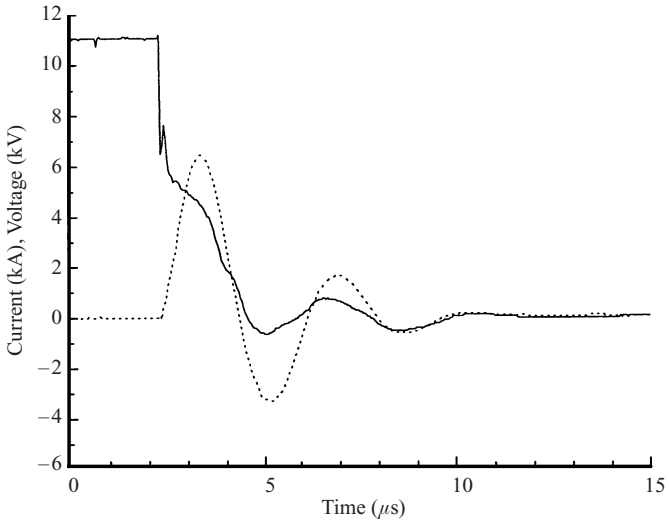

Figure 2. Current (·····) and voltage (——) oscillograms of a water arc.

of the voltage drop across the external circuit portion. Part of this drop is likely to be due to the initial ionization.

3. Fog evidence

Figure 3 is a series of photographs showing the emergence of fog from a water arc accelerator barrel (Graneau and Graneau 1996). In this shot the energy in the capacitor was 40 J. For comparison, a match liberates about 200 J of heat. The camera was operated at 10000 frames/s. Hence the time interval between exposures was 100 μs, of which the shutter was open for the first 20 μs. The high-speed photography was performed at Oxford University.

Water vapour and steam are invisible in air. Relatively large drops of water and films are transparent. They show up on photographs only as thin lines of light, which represent reflections from the water surfaces. The uniform whitish-grey appearance of fog and clouds is due to light scattering by a high density of very small droplets. Hence the photograph in Fig. 3 provides conclusive proof that fog emerged from the accelerator barrel. As the heat evolved in these experiments is insignificant and the electrodynamic forces are too weak, the only way in which the fog explosion can be explained is by the sudden mutual repulsion of fog droplets.

A more dramatic fog explosion is shown by the two video frames of Fig. 4. They relate to a capacitor discharge of 324 J of energy with a $\frac{1}{4}$-inch thick plywood square initially resting on the accelerator muzzle. The fast fog is seen to penetrate the plywood and still pierce the atmosphere at supersonic speed, as indicated by the conical tip of the jet more than one metre above the muzzle. The second frame of Fig. 4 shows the hole punched through the plywood board as the latter lifts off the accelerator.

The mechanism of condensation of water vapour in air is the most prolific fog producer on Earth. It is a slow process, and cannot generate an equivalent quantity of fog to that in the few microseconds of a water arc explosion. In the

https://doi.org/10.1017/S0022377898007089 Published online by Cambridge University Press

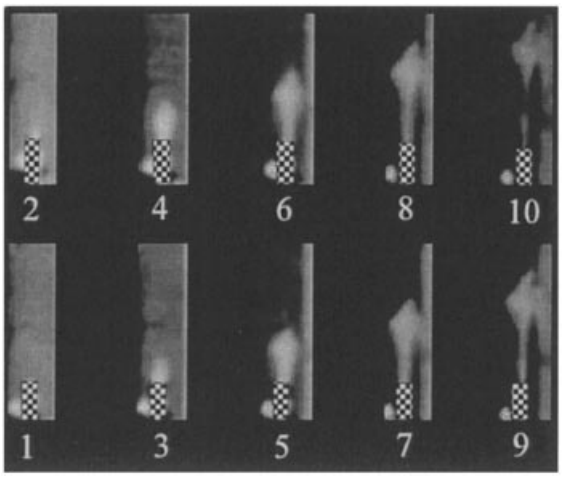

Figure 3. High-speed photographs of the development of the fog plume (10000 frames/s).

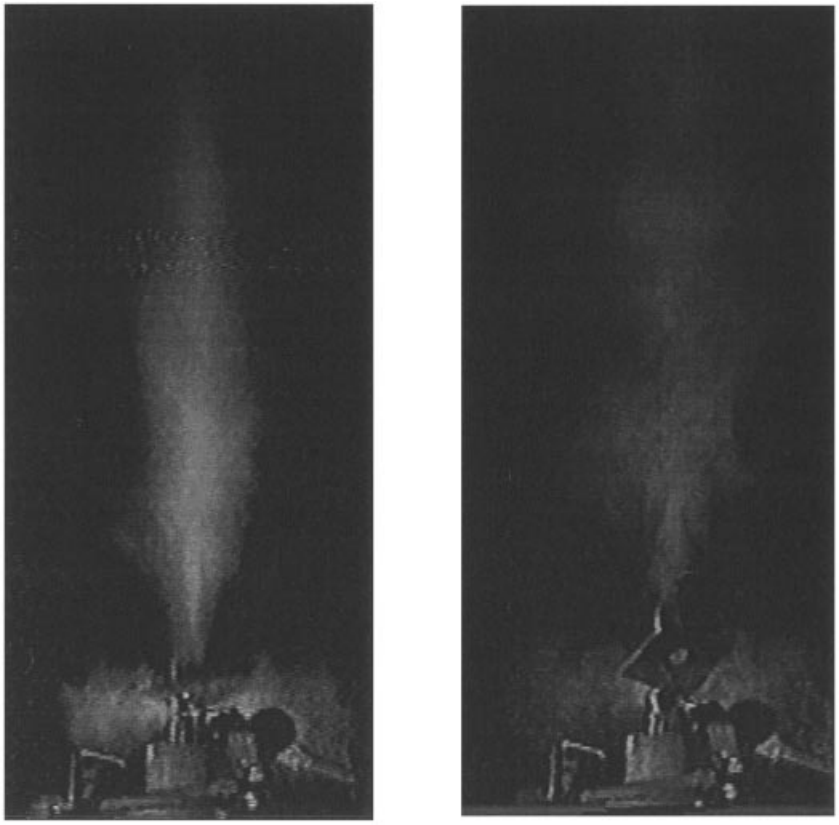

(*a*) (*b*)

Figure 4. Two video frames from a BBC TV programme in which Richard Hull of the TCBOR laboratory, Richmond, VA demonstrated water arc explosions: (*a*) supersonic fog jet penetrates plywood sheet; (*b*) hole punched through sheet by fog jet.

https://doi.org/10.1017/S0022377898007089 Published online by Cambridge University Press

early formative stage of the arc, the fog density must approach that of liquid water, and is therefore up to 300000 times as great as the fog density of clouds in the atmosphere, which is 3 g m^{-3}.

It is difficult to think of any other way of creating the dense fog than by mechanically tearing the liquid apart into tiny fragments. These fragments are the fog droplets, probably ranging in size from 1 to 100 μm in diameter, as deduced from the fact that they float in air. For want of any other force known to be present in the explosion, the tearing force has to be of electrodynamic origin. The directions of the Lorentz forces are not such that they could split water into fog droplets. However, Ampère tension (Graneau and Graneau 1996) is well qualified to accomplish this task.

The best-known consequence of Ampère tension in metallic conductors is the phenomenon of wire fragmentation. In liquids and plasmas it leads to plasma bead formation, which has been observed in plasma focus fusion and other filament fusion processes. All these facets of the action of Ampère tension are fully described in Graneau and Graneau (1996).

In any case, the existence of the surface tension of water actually requires the presence of tearing forces. The surface tension γ of water at 20 °C is 72.75 dyn cm^{-1}. It turns out that surface tension energy per unit area has the same dimension as surface tension per unit edge, and is numerically equal to it, so that

$$\begin{aligned}\gamma &= 72.75 \text{ dyn cm}^{-1} = 72.75 \text{ erg cm}^{-2} \\ &= 72.75 \times 10^{-7} \text{ J cm}^{-2}. \end{aligned} \tag{14}$$

It is known that the surface energy changes with the age of the surface. As a result, for the first 10 ms after fog formation, the surfaces are likely to store more energy than indicated by (14). The fog mass generated in our experiments was typically 0.2–0.5 g. Let us thus calculate the additional surface energy required to convert 1 g (1 cm^3) of water into fog. If the droplets are all of the same diameter d, measured in cm, then the number n of droplets generated will be

$$n = \frac{6}{\pi d^3}. \tag{15}$$

Fog droplets are said to be between 10^{-4} and 10^{-3} cm in diameter. Hence the number of droplets lies in the range from 1.9×10^6 to 1.9×10^{12} per gram of bulk water. The total new surface energy for drops of the same size is

$$E_s = \gamma n \pi d^2. \tag{16}$$

For the two extreme droplet diameters of 10^{-2} cm and 10^{-4} cm, this comes to 4.37 mJ and 437 mJ respectively. Hence the part of E_7 in the energy flow diagram of Fig. 1 that must supply surface-tension energy is only a fraction of one joule. Ampère tension forces can comfortably meet this energy demand according to (6) with $k = 200$ (see the discussion in Sec. 1).

4. Type B accelerator results

Some of the various water accelerator designs that have been used since 1983 are described in Graneau and Graneau (1996). A design that has been called the type B accelerator is shown in Fig. 5. To determine the fog-jet momentum, a

https://doi.org/10.1017/S0022377898007089 Published online by Cambridge University Press

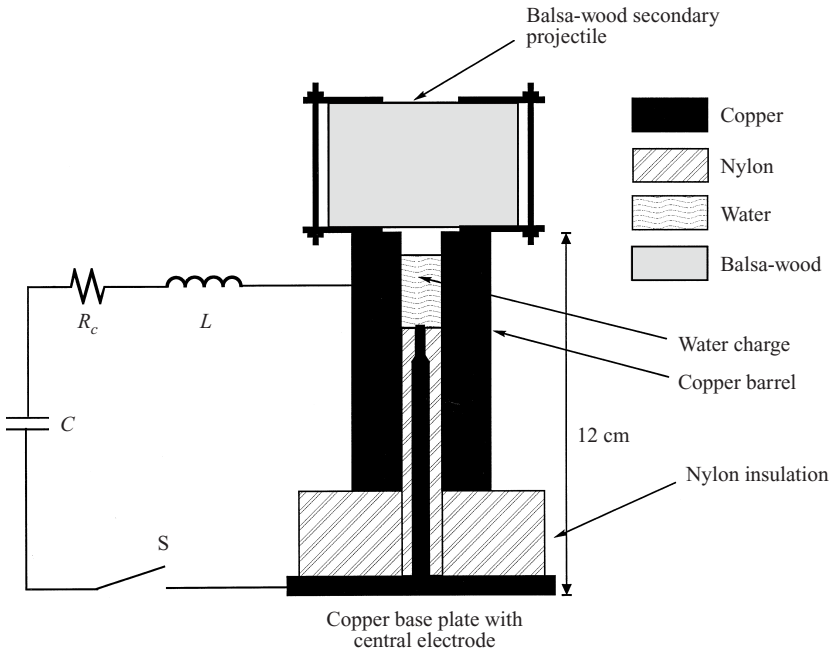

Figure 5. Type B accelerator with secondary projectile and discharge circuit.

secondary projectile consisting of balsa wood stands on the accelerator barrel. The balsa wood is given mechanical strength by steel washers at the top and bottom, held tightly by screws outside the wood. The dry mass of the projectile is denoted by M, and was usually around 64 g, while the mass of the fog absorbed in the wood is denoted by m. A capacitor, $C = 9.565\,\mu\text{F}$, is charged to the voltage V_0 and then discharged through the accelerator by closing the switch S. An oscilloscope records the discharge current $i(t)$ as in Fig. 2.

The throw height h of the secondary projectile is measured with a freeze-frame video camera. This defines the initial velocity of the projectile as

$$v_0 = (2gh)^{1/2}, \tag{17}$$

where g is the acceleration due to gravity. Because of momentum conservation, the average velocity u_{av} of the fog mass that penetrated deep into the balsa wood is given by

$$u_{\text{av}} = \frac{(M+m)\,v_0}{m}. \tag{18}$$

In some shots, not all of the capacitor energy is discharged, leaving a residual voltage V_r on the capacitor terminals. Hence the net energy actually discharged into the circuit is

$$E_2 = \tfrac{1}{2}C(V_0^2 - V_r^2). \tag{19}$$

The kinetic energy of the fog jet is

$$E_{12} = \tfrac{1}{2}mu_{\text{rms}}^2. \tag{20}$$

Neither the mass distribution of the fog droplets nor their velocity distribution are known. However, as on previous occasions, the simplifying assumption is

https://doi.org/10.1017/S0022377898007089 Published online by Cambridge University Press

Table 1. Results of reported water arc experiments.

Shot no.	V_0 (kV)	E_2 (J)	$E_3+E_5+E_6$ (J)	u_{av} (m s^{-1})	E_{12} (J)
SP12	10	28.3	20.5	258	21.0
SP13	9	22.9	17.5	273	21.5
SP14	12	40.7	31.2	235	221.5
SP15	12	40.7	31.2	244	17.8
SP16	12	40.7	32.2	229	20.9
SP17	10	28.3	22.2	172	13.0
SP18	10	28.3	22.2	258	21.8
SP19	10	28.3	22.2	274	23.1
SP20	10	28.3	22.2	218	17.8
SP21	10	28.3	22.2	191	16.1
SP22	10	28.3	22.2	251	19.7
SP23	12	39.8	31.2	243	22.3
SP24	12	39.8	31.2	306	29.2
SP25	12	39.8	31.2	275	28.5

made that the droplets are of equal size and their velocity distribution is half a cycle of a sine wave. This results in

$$u_{rms} = 1.11\ u_{av}. \tag{21}$$

Table 1 lists the results of 14 shots. In all cases the initial water charge was 1.5 ml of distilled water at room temperature.

5. Discussion of results

The kinetic energies of the fog jets, E_{12}, have been derived from the dry and wet weights of the balsa wood secondary projectile, M and $M+m$, the throw height h and (17)–(21). Table 1 shows these energies to vary between 13.0 and 29.2 J. Take shot SP24 with the largest kinetic-energy output. For this shot, the fog mass $m = 0.504$ g and its average velocity came to $u_{av} = 306.4$ m s^{-1}. This resulted in an impulse exerted on the secondary projectile of $P_{12} = mu_{av} = 0.154$ N s. The action integral of this shot was $\int i^2\,dt = 157$ A^2 s. With the Ampère force factor, $k \leqslant 200$, (6) gives $P_7 \leqslant 3.14 \times 10^{-3}$ N s. The impulse and energy ratios are therefore $P_{12}/P_7 \geqslant 49.0$ and $E_{12}/E_7 \geqslant 2401$. Hence $E_7 \leqslant 12.1$ mJ, which is negligible compared with $E_{12} = 29.2$ J and demonstrates that virtually all of the kinetic energy developed by the explosion must be internal water energy. Note that the calculated value of E_7 is in line with the estimated surface-energy increase required for the formation of a large number of fog droplets, as discussed at the end of Sec. 3.

In spite of the gain in internal water energy, the overall ratio E_{12}/E_2, is less than unity because of the five loss components indicated on Fig. 1. A circuit-loss $E_3+E_5+E_6$ estimate was made with the current oscillogram of shot SP24. This indicated a ringing frequency of 384 kHz, which, together with the capacitance $C = 0.565\ \mu$F, gave a self-inductance $L = 0.3\ \mu$H. The decay time constant $T = 3.5\ \mu$s and the action integral came to $\int i^2\,dt = 157$ A^2 s. From (2), the damping resistance was found to be $R = 173$ mΩ. This resulted in a total damping loss of $R\int i^2\,dt = 27.2$ J. To this should be added at least 10% of

https://doi.org/10.1017/S0022377898007089 Published online by Cambridge University Press

$E_2 = 39.8$ J to account for the initial ionization loss, to arrive at the circuit-loss figure of around 31 J for the 12 kV shots in Table 1. By adding the approximate circuit loss to the fog kinetic energy E_{12}, it is found that the sum is greater than the input energy. This can be expressed as

$$E_{12} + (E_3 + E_5 + E_6) > E_2, \tag{22}$$

proving once more the involvement of internal water energy. This argument ignores further significant energy losses such as E_{10} and E_{11} of Fig. 1. It is not out of the question that E_{11} is as large as E_{12}.

In order to utilize the internal water energy for electricity generation, large reductions in circuit loss and barrel losses have to be achieved. Our objective has been to prove the liberation of internal water energy. We have made no effort to optimize the process.

6. Renewable water energy cycle

Figure 6 is a block diagram showing the circulation of water molecules through the fog accelerator, whence they dispersed into the atmosphere and condensed to raindrops in clouds. The high-voltage capacitor energy E_C is known accurately. The low-grade heat losses E_h and the fog kinetic energy E_k have been measured with adequate precision. From the measurements, we know that

$$E_k \gg E_C - E_h. \tag{23}$$

Hence internal water energy must be contributing to the fog explosions. Other than the capacitor energy, the only external energy supplied to the experiment is solar heating of the fog and atmospheric water vapour. Accepting that energy has to be conserved, this proves that the fog explosions are, indirectly, driven by solar energy. The process is renewable, and does not pollute the atmosphere or contribute to global warming.

Owing to thermal agitation, the molecular structure of the water is continuously fluctuating. This structure, that is the mutual arrangement of the H_2O dipoles, is the subject of intense research elsewhere. All we can do with respect to the H_2O–H_2O bonding is to speculate what the relevant energy processes may be.

In our present state of knowledge, the most likely explanation of the fog explosions is that they are caused by the liberation of intermolecular bonding energy when the bulk water is transformed into tiny fog droplets. This bonding is caused both by hydrogen bonds and the weaker van der Waals forces, and the energy stored by the bonds (which means the energy that must be supplied to break them) is roughly equal to the latent heat of water, and is found to be 2.3 kJ g^{-1} at 20 °C.

The creation of a large number of droplets is thought to be caused by the mechanical effects of the electrodynamic forces in the arc discharge. A lack of significant temperature change rules out a thermal mechanism for droplet creation. A certain amount of mechanical energy is thus used to create the droplets, and is consequently stored as surface tension energy. However, the molecules in the small droplets now have significantly fewer neighbours than in the bulk water, and can orientate themselves more easily into lower-energy states. These lower energies imply that the bonds become stronger, thus

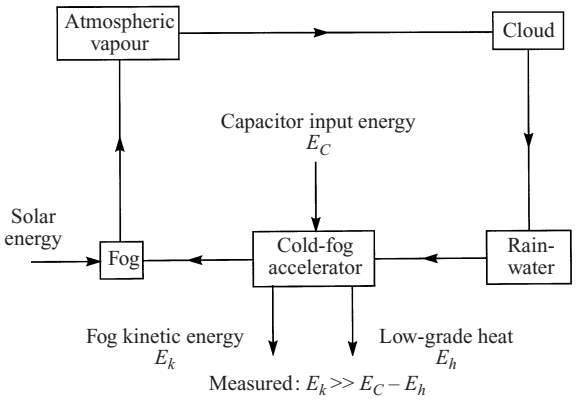

Figure 6. Renewable water energy cycle.

requiring more energy to break them. This bond-redistribution behaviour is normally observed in thin films of water, and is called vicinal water (Adamson 1990). Recent results of inelastic incoherent neutron scattering (IINS) experiments in water and ice (Li and Ross 1993; Li 1996) have revealed that in ice there are two molecular optic peaks in the IINS spectrum at 28 and 37 meV (24 and 32 meV for liquid water). The two peaks can be explained by a model involving two types of hydrogen bond (Li and Ross 1993), and they are referred to as the weak and strong bonds respectively. If in the newly formed droplets some of the weak bonds drop to the strong bond energy in a quantum shift, there will be a consequent release of kinetic energy causing the explosion of the vicinal water droplets. The same is true if either a weak or strong bond is formed between two molecules that were previously only held together by van der Waals forces. If enough of these bonds change energy level then more kinetic energy could be released than the mechanical energy used to create the droplets in the first place, thus liberating a net amount of energy from the original bulk water. In order to restore the droplets to their normal water state, some energy input is required; in our case this must come from atmospheric heat, and this process can occur away from the explosion region and over a much longer time. Therefore the explosion is conjectured to be a sudden release of energy from the water that was originally stored by atmospheric heat and is later restored to the water after the explosion also by atmospheric heat, while in the meantime the net gain in kinetic energy can be harnessed for useful means.

The following argument should clarify how atmospheric heat is stored in the bulk water. When molecules condense into a droplet, the system is heated by the kinetic energy produced by the decrease in potential energy from (*a*) the molecule and droplet infinitely far apart and (*b*) in the bonded position, and represents the quantity of energy normally referred to as latent heat. This process represents the creation of atmospheric heat as a result of collisions of the incoming molecule (attracted by the droplet) with other vapour molecules. If the molecule arrives at the droplet with a non-zero kinetic energy, this will heat the droplet additionally. Similarly, when two molecules inside the droplet form a hydrogen bond or change from a weak to a strong bond, the drop in potential energy must also create an increase in kinetic energy. These shifts

https://doi.org/10.1017/S0022377898007089 Published online by Cambridge University Press

represent the liberation of energy stored in the water that must have been there to allow weak bonds and unbonded molecules to exist. It is thus conjectured that the original source of this stored energy is heat supplied from the atmosphere, and this makes it possible to effectively tap the solar energy that is stored in normal bulk water.

References

Adamson, A. W. 1990 *Physical Chemistry of Surfaces*, p. 280. Wiley, New York.

Azavedo, R. *et al*. 1986 Powerful water-plasma explosions. *Phys. Lett*. **117A**, 101.

Chen, S. H. 1989 Quasi-elastic and inelastic neutron scattering and molecular dynamics of water at supercooled temperature. *Proceedings of NATO Advanced Study Institute on Hydrogen-Bonded Liquids* (ed. J. C. Dore and J. Teixera), p. 289.

Früngel, F. 1948 Zum mechanischen Wirkungsgrad von Flussigkeitsfunken. *Optik* **3**, 125.

Graneau, P. 1996 Gaining solar energy from ordinary water. *Proceedings of World Renewable Energy Congress IV*, *Denver*, *CO*, *June 1996*.

Graneau, P. and Graneau, N. 1985 Electrodynamic explosions in liquids. *Appl. Phys. Lett*. **46**, 468.

Graneau, P. and Graneau, N. 1996 *Newtonian Electrodynamics*, pp. 249–271. World Scientific, Singapore.

Li, J. 1996 Inelastic neutron scattering studies of hydrogen bonding in ices. *J. Chem. Phys*. **105**, 6733.

Li, J. and Ross, D. K. 1993 Evidence for two kinds of hydrogen bond in ice. *Nature* **365**, 327.

Northrup, E. F. 1907 Some newly observed manifestations of forces in the interior of an electric conductor. *Phys. Rev*. **24**, 474.

Wilson, F. W. (ed.) 1964 *High Velocity Forming of Metals*, pp. 77–93. Prentice-Hall, Englewood Cliffs, NJ.